Front. Chem. China 2011, 6(3): 173–189
DOI 10.1007/s11458-011-0254-5

REVIEW ARTICLE

Solid state NMR study of hydrogen bonding, miscibility, and dynamics in multiphase polymer systems

Weigui FU (✉)[1] and Pingchuan SUN[2]

The application of solid state NMR (SS NMR) to the study of multiphase polymer systems is growing rapidly. This article aims to provide an overview of the current state of development of this field, paying particular attention to the study of hydrogen bonding in hydrogen-bonded polymer materials through SS NMR investigations. The effection of hydrogen bonds on the miscibility, phase separation and dynamic behavior of selected systems will also be discussed, based on work during the last 10 to 15 years.

Keywords solid state NMR, hydrogen bonding, miscibility, dynamics, multiphase polymer

1 Introduction

Multiphase polymers with nanostructures, such as polymer blends, organic/inorganic hybrids, biologic macromolecules, and block copolymers, are being paid much attention as an important field in polymer science [1,2]. Since the physical and chemical properties of the materials are strongly influenced by the intimacy of mixing, a better understanding of miscibility and phase behavior of polymer blends and composites are essential for the development of materials science. It is well known that hydrogen bonding (X-H…Y), characterized as a relatively weak interaction involving a proton donor X, a hydrogen, and a proton acceptor Y, plays an important role in determining the structures and properties of a range of materials [3–6], ranging from inorganic to biological systems. Through introducing the intermolecular hydrogen bonding [7,8], we can obtain miscible polymer blends, build new molecular self-assembled materials and 'layer by layer' polymer film [9–14], make functional ion-exchange resins for adsorption and separation, and control the peptide secondary structures and miscibility behavior of peptides with resins [15]. Meanwhile, high property polymer/inorganic particles composites can be tailored by the incorporation of inter-associated hydrogen bonds [16–18]. Furthermore, hydrophilic polymer or proteins may be swollen by the adsorption of water through the formation of hydrogen bonding with water, thus induces considerable mechanical and chemical changes [19–21]. So it is a topic of vital scientific research for developing new methods to determine the hydrogen bonding interactions in multiphase polymers, and illustrating the relationship between the weak molecular interactions to the polymer condensed structures and dynamic behavior at molecular scale.

Nuclear magnetic resonance (NMR) is sensitive to the local environment and is complementary to the longer range structure information provided by imaging and diffraction techniques. Unlike most other techniques, solid state (SS NMR) measurements, such as ^{1}H spin diffusion [22,23], relaxation times observation [24,25], offer a very powerful and convenient tool for studying the microphase structures, segmental dynamics of multiphase polymeric materials [26,27], and can provide detailed insights into the properties of hydrogen bonded systems [28]. It has become increasingly common to supplement the experimental data with adequate numerical simulations. Ab initio calculations are often useful to divide factors that influence chemical shifts into "through-bond" effects that derive from the local chemical environment, and longer range effects arising from non-bonded intra or intermolecular interactions, so they are becoming increasingly popular for solid state SS NMR experiments [29]. To date, some theoretical researches on small drug design [17] and solid acid catalysis [18] mainly used quantum calculation for the NMR isotropic chemical shifts. Although isotropic shift can illustrate proton states and provide information on the strength of hydrogen-bonding interactions as well as molecular structures, for the ^{15}N and ^{1}H chemical shifts of some solid amino acids did not move obviously with the change of its hydrogen-bonding environments.

With the development of quantum calculation on the NMR chemical shifts, chemical shift anisotropy (CSA) will become a new effective method for studying molecular conformations and interactions [18,35,36]. MeDermott's group first investigated the hydrogen-bonding interactions in amino acids by calculating the CSA of hydrogen-bonding acceptors [37]. By now, the work on studying hydrogen bonding interactions in multiphase polymers combined CSA quantum calculation and solid state SS NMR measurements is seldom reported. These methods shall be discussed in the following sections.

Received September 18, 2011; accepted September 23, 2011
1. Department of Materials Science and Engineering, School of Materials Science and Engineering, Tianjin Polytechnique University, Tianjin 300160, China
2. Key Laboratory of Functional Polymer Materials, Ministry of Education, Institute of Polymer Chemistry and College of Chemistry, Nankai University, Tianjin 300071, China
E-mail: tjfwg@hotmail.com

©Higher Education Press and Springer-Verlag Berlin Heidelberg 2011

In addition, this weak interaction affects the dynamic behavior of polymer chains in multiphase samples. Molecular dynamics of the polymer chains are known to play an important role for understanding correlations between microstructure and its properties. A large number of NMR works have been published and some of them were reviewed [38,39]. The importance of solid state SS NMR techniques for the study of dynamics is due primarily to its ability to detect correlation times of motion in the range 10^{-1} to 10^{-10} s [40]. Different solid state SS NMR experiments in low resolution (line-width, spin-diffusion) [41,42] and high resolution (line-shape analysis at variable temperature [43], relaxation time studies [44–46], CSA analysis [47], etc.) can be customized for detecting and quantifying molecular motions involving individual groups or entire molecules. The classical NMR approaches for investigating dynamic information are the determination of relaxation times [48] and ^{2}H NMR [49], with the latter being sensitive to the amplitude of segmental motion, geometry property and time scale. However, it is difficult to distinguish one chemical group from another, which can be obtained by 2D WISE experiment [50–55]. Another common experiment is DIPSHIFT [56], which measures the heteronuclear dipolar coupling between a ^{1}H spin and a heteronuclear spin *S*. While the DIPSHIFT experiment provides information on the motional amplitude, it typically does not yield the detailed information on geometry of motion. In recent years, a new NMR method has been developed by deGroot [55] and Hong et al. [57] to detect the strength of ^{13}C-^{1}H dipolar coupling and the distance of nuclei, which use LG-CP technique to remove ^{1}H-^{1}H homonuclear dipolar interaction and ^{1}H spin-diffusion while obtaining the strength information of ^{13}C-^{1}H dipolar interaction effectively. Combination with computer simulation, LG-CP technique can obtain the information on the molecular motion amplitude, geometry property and time scale, which is more plentiful than that of the above classic methods. To date, several approaches have been developed to characterize ^{13}C-^{1}H dipolar interaction, and have been widely applied to research the liquid crystals and membrane proteins [58–61]. For rigid polymer system, polarization inversion spin exchange at the magic angle (PISEMA) experiment was used to probe strong ^{13}C-^{1}H dipolar interaction and determine heteronuclear (^{1}H-^{13}C) distance of molecules and molecular torsion angles.

In this review, we would like to present investigations of multiphase polymer systems with hydrogen bonding by solid state SS NMR. Special emphasis will be laid on applications of recently developed and advanced NMR methods available to a spectroscopist for the complete understanding of the interplay of intermolecular interactions with the miscibility, phase behavior and dynamics of molecules in polymer materials with a focus on polymer blends and polymer/clay nanocomposites.

2 Hydrogen bonding interaction

Hydrogen bonding plays a fundamental role in structure, function and dynamics of multiphase polymer materials for its directionality, specificity, strength and selectivity [62–64]. Thus, a variety of methods were used to obtain the information about hydrogen bonding in polymer systems, such as IR [65–67] spectroscopy, Raman spectroscopy [66,68,69], NMR [70–72] spectroscopy, neutron diffraction [73,74], single-crystal X-ray diffraction [75] and so on. Among these experimental methods, IR and NMR spectroscopy are the most effective and widely used methods to characterize the hydrogen bonds in the systems of multiphase polymer. Solid-state NMR is able to investigate the microscopic environment at each individual site in a solid material and has therefore emerged as a powerful technique especially in solid systems lacking the order or homogeneity for polymers. Therefore, it has also been used as one of the most powerful means for probing miscibility, phase behavior, intermolecular interaction and molecular motion in polymer blends. However, these techniques have some intrinsic limitations and cannot be universally applied. Furthermore, quantum chemistry calculation methods are also employed to investigate hydrogen bonds theoretically [32,76].

Several excellent reviews on hydrogen bonds and their effects on the microstructures [77,78] and physical properties of various materials such as polymer blends [79–81], peptides and polypeptides [78], and crystal supramolecular systems [82] and so on, are available. Here we briefly present some new experimental and theoretical NMR studies on the main parameters related to the hydrogen bonding interactions in the solid state: (a) chemical shift, (b) double quantum transitions, (c) chemical shift anisotropy (CSA), (d) ab initio calculations.

2.1 ^{1}H CRAMPS NMR

Hydrogen bonding interactions between polymer and biomacromolecules (such as hydrogels or proteins) and water play a dominant role in the determination of the structure and good mechanical properties of materials. Basic information about hydrogen bonding can be gained from the solid-state ^{1}H chemical shifts. High-speed magic-angle spinning (MAS) technology at spinning frequencies of 25–30 kHz allows the location of chemical shifts of hydrogen bonded protons. ^{1}H SS NMR is still the most useful technique due to its high sensitivity to the hydrogen bonding strength and the state of

water [83–88], although the strong ^{1}H-^{1}H dipole-dipole interaction veils many important structural information. Fast MAS [89] or combined rotation and multiple-pulse spectroscopy (CRAMPS) [90–92] techniques are commonly used to remove the homogeneous line broadening of protons to obtain high-resolution solid state ^{1}H NMR spectra. The continuous phase modulation techniques proposed by Emsley's group provided better ^{1}H-^{1}H homonuclear dipolar decoupling at high sample spinning frequencies vs. traditional CRAMPS methods [93]. To observe the information from the proton chemical shift, variable temperature ^{1}H MAS NMR can be used to determine the temperature dependence of various types of hydrogen bonds. Sun's group systematically elucidated different types of hydrogen bonds and their temperature dependence, as well as water-polymer interaction in hydrated PAA using 1D and 2D ^{1}H CRAMPS solid-state NMR experiments based on continuous phase modulation technique in the temperature range from 25 to 110°C [94].

It is generally accepted that three different states of water are present in PAA polymers, known as "bound," "intermediate," and "free" water, respectively. There are different types of protons and they may be associated or not associated with hydrogen bonds in the hydrated PAA samples. They are denoted as the following abbreviations: H_{DM} represents the protons of hydrogen bonds between COOH groups including cyclic and open COOH dimers; H_{FR} denotes the non-hydrogen-bonded protons on isolated COOH or open COOH dimer; H_{PW} represents the COOH protons which can form hydrogen bonds with water; and H_W represents the water protons which can form hydrogen bonds with polymer (bound water) or with other water molecules (intermediate water). As shown in Fig. 1, there exist three types of hydrogen bonds which are associated with H_{DM}, H_{PW} and H_W protons, respectively. The different chemical environment of the protons shown in Fig. 1 may significantly affect their ^{1}H chemical shift. On the other hand, it is expected that the protons in different chemical environments should exhibit difference in the molecular mobility.

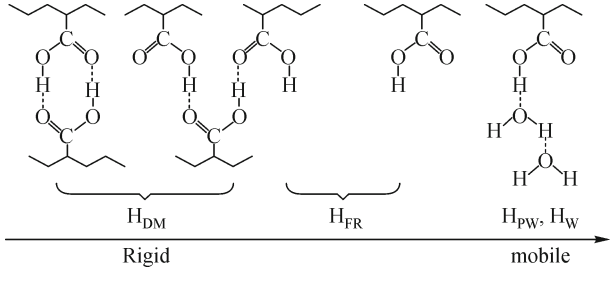

Figure 1 Schematic illustrations of different types of protons and their associated hydrogen bonds (dotted line) in hydrated PAA [94].

The solid-state ^{1}H PM-CRAMPS NMR spectra of PAA0 (35 wt% solution sample) at different dehydration time from 1 day to 5 days (i.e., PAA1, which contains about 7 wt% residual water) at room temperature with a relative humidity (RH) of 80% are shown in Fig. 2. Fig. 2(a) shows that one strong peak at 7.1 ppm and one weak and broaden peak at 2.0 ppm can be clearly observed for the 1-day dried sample, which should be assigned to the overlapped signals of the methine and methylene protons of PAA. And the strong peak at 7.1 ppm should be reasonably assigned to the protons of large cluster of water molecules (H_W) that are mutually hydrogen bonded and/or also interact with the COOH side groups, as well as the COOH groups undergoing fast chemical exchange with water (H_{PW}). It is observed that the signal of water at 7.1 ppm gradually broadens out and shifts to 8.5 ppm with the increase of the dehydration time from 1 to 5 days, which indicates that the chemical shift of water signal depends strongly on the water content. This is also a clear evidence of the chemical exchange between water and PAA COOH groups. The decreasing and broadening of the water peak shown in Fig. 4 also suggest that the amount of the intermediate water decreases while that of the bound water increases with an increasing dehydration time. It is noteworthy that a new broad peak at about 10–13 ppm occurs after 2 days' dehydration and increases with further dehydration, while the chemical shift of this broad peak keeps unchanged during further hydration. Since dehydration cannot result in the increase of H_{PW} signals, the new broad peak at 10–13 ppm should be reasonably assigned to the H_{DM} and H_{FR} instead of the H_{PW} protons. The above result suggests that the stable hydrogen bonds between COOH groups related to DM can

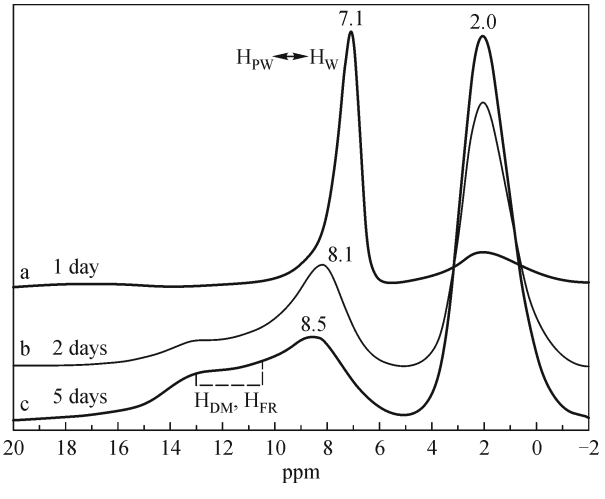

Figure 2 ^{1}H PM-CRAMPS NMR spectra of PAA0 (representing PAA 35 wt% solution sample) at dehydration time of (a) 1 day, (b) 2 days, and (c) 5 days (PAA contains about 7 wt% residual water, denoted as PAA1).

easily form in dehydrated PAA and are unfavorable in highly hydrated PAA.

2.2 Double quantum (DQ) NMR

In recent years, noncovalent interactions in macromolecular, organic-inorganic hybrid materials, and supramolecular systems have been studied by a variety of high-resolution homonuclear (^{1}H-^{1}H) and heteronuclear (^{1}H-^{13}C, ^{15}N) multiple quantum (MQ), in particular double quantum (DQ) solid-state NMR techniques based on through-space dipolar interactions between nuclei which are close in space [82,95–99]. The largest MQ signals arise from strongly dipolar-coupled protons. The dipolar coupling interaction is usually averaged by fast MAS, and therefore it must be reintroduced by a suitable pulse sequence to simultaneously detect strong ^{1}H-^{1}H dipolar couplings and enhance the ^{1}H chemical shift resolution. Recently, the ^{1}H double quantum (DQ) NMR spectroscopy under fast MAS NMR at very high magnetic field and recoupling techniques using back to back (BABA) sequence (as shown in Fig. 3(a)) was introduced for probing dipolar couplings [100–102]. The BABA experiment correlates a dipolar filtered ^{1}H single quantum (SQ) dimension to a ^{1}H double quantum (DQ) dimension, as shown in Fig. 3(b) (the slope of the 2D experiment is set to 2). For a given spin system exhibiting protons strongly coupled by the homonuclear dipolar interaction (Fig. 3(b)), the BABA experiment is interpreted as follows: a pair of coupled protons exhibiting different chemical shifts δ_1 and δ_2 is characterized by two off-diagonal correlation peaks located at (δ_1, δ_2) in the SQ dimension and ($\delta_1 + \delta_2$) in the DQ dimension. For protons exhibiting the same chemical shifts δ_i, one unique on-diagonal correlation peak is observed at (δ_i) in the SQ dimension and ($2\delta_i$) in the DQ dimension. Such a sequence has been previously used for the detailed study of supramolecular systems involving hydrogen bonding and sol-gel derived materials [103–107].

2.3 ^{17}O solid-state NMR

The oxygen atom is probably the most chemically and biologically important element on earth which contains about 50% by weight of oxygen. Oxygen forms compounds with all elements except for a few noble gases and metals. Therefore, it is valuable for oxygen-17 to probe both structure and function of oxygen-containing compounds. Table 1 lists some useful data of the ^{17}O nucleus. It is a nuclear spin ($I = 5/2$), and has a moderate electrical quadrupole moment ($Qe = -2.63 \times 10^{-30}$ e m^2), a very small magnetogyric ratio ($\gamma = -3.688 \times 10^{-7}$rad. T^{-1} s^{-1}), a low natural abundance (0.037%) and an extremely low absolute sensitivity compared to that of ^{1}H (1.1×10^{-5}). So, generally, the ^{17}O NMR spectra are of low sensitivity and complex. It is, however, of great interest to use oxygen, which is located at strategic molecular sites, and gain inter- and intramolecular interactions imformation which is difficult or impossible to obtain using other techniques. The ^{17}O NMR parameters, i.e., isotropic shielding (δ_{iso}), principal elements of the ^{17}O shielding and electric field gradient tensors and transverse and longitudinal relaxation times can be considered as excellent means for probing the structure, bonding and dynamics of oxygen containing compounds [109].

One of the core interests in applying ^{17}O solid-state NMR is to probe hydrogen bonding. Oxygen atoms are usually optimally located to monitor any hydrogen bonds, and due to its quadrupolar nature, it should be very sensitive to any changes of the strength of such interactions [110]. X-ray crystallographers have stated that the N-H…O-C hydrogen bond is a universal feature of amino acid aggregation in the

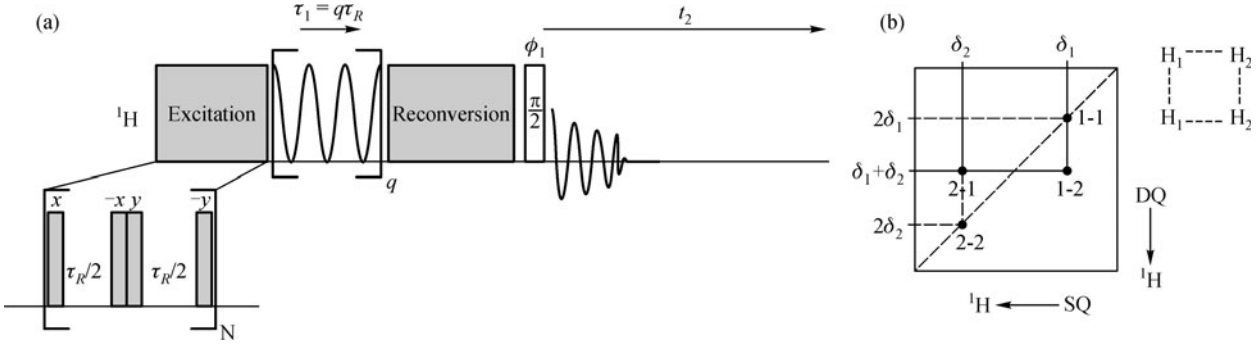

Figure 3 a) 2D ^{1}H–^{1}H DQ-SQ experiment using back to back (BABA) pulse scheme for the excitation and reconversion of DQ coherence [108]; b) Schematic system of four dipolar coupled (close in space) ^{1}H nuclei (H_1…H_1, H_1…H_2 and H_2…H_2). For identical chemical shifts, a unique on-diagonal correlation peak is observed. For different chemical shifts, two off-diagonal correlation peaks are observed [107].

Table 1 Magnetic properties and nuclear magnetic resonance parameters of the oxygen-17 nucleus (Adapted, with permission, from NMR-Basic Principles and Progress. Copyright 1981, Springer.)

Property		Units
Spin number	5/2	
Nuclear magnetic moment	−1.893997	Nuclear magneton
Magnetogyric ratio	-3.688×10^{-7}	Rad.s^{-1}T^{-1}
Resonance frequency (at 9.395 T)	54.227	MHz
Chemical shift range	>2500	ppm
Quadrupole moment	-2.63×10^{-30}	e m^2
Nuclear quadrupole coupling constant range	−10 to + 14	MHz
Relaxation times	<0.2	s
Natural abundance	0.037%	
Relative sensitivity per nucleus (^{1}H = 1)[a)]	2.9×10^{-2}	
Absolute relative sensitivity at natural abundance (^{1}H = 1)[b)]	1.1×10^{-5}	

a) Relative to proton, at constant field, for equal number of nuclei;
b) Product of relative sensitivity and natural abundance

solid-state [111]. Hydrogen bonding for carbonyl groups often results in large upfield ^{17}O chemical shifts [112]. Furthermore, it seems that the whole network of the hydrogen bonds and the general geometry of the local environment (i.e., secondary structure) has also to be taken into consideration. In poly(l-alanine), the α-helix and β-sheet forms show a difference in δ_{iso} of 33 ppm, which is related to the different hydrogen bonding of these two secondary structures [113].

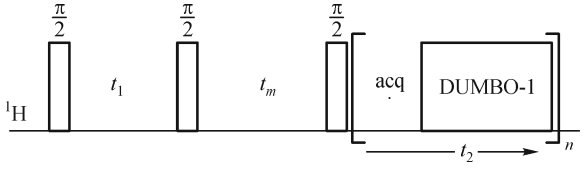

Figure 4 Pulse sequence of 2D ^{1}H-^{1}H spin-exchange NMR experiments recorded with DUMBO-1 homonuclear decoupling multi-pulse during t_2

2.4 Intermolecular hydrogen bonds by 2D ^{1}H-^{1}H spin-exchange

Traditional two-dimensional nuclear Overhauser effect spectroscopy (NOESY) has been used to characterize the intermolecular interactions in the mixture of miscible blends. The interacting groups can be identified and the forces that lead to molecular level miscibility can be determined by such high a resolution technique [114,115]. While the nuclear Overhauser effect (NOE) is routinely used in solution for structural and conformational analysis, it is rarely considered for pure solid materials. Ernst et al. used two dimensional (2D) ^{1}H-^{1}H spin-exchange experiments to probe the polymer-polymer miscibility [116–118].

To confirm the thermal-treating effect on the diffusion and miscibility of the powder blend samples, 2D ^{1}H-^{1}H spin-exchange experiments were performed for PMMA/PVPh powder blends (denoted as Blend0) and its thermal-treated samples under different annealing time at 220°C in our previous work [119]. This work was desired to extend NOE measurements to solid polymer blends in a high-resolution multi-pulse and magic-angle spinning mode for the first time. The ^{1}H-^{1}H spin-exchange spectra were obtained by the pulse sequence as shown in Fig. 4 at different mixing time (t_m) of 0.5, 1.0 and 2.0 ms. 2D experiments were taken with 100 data points along t_2 and with 128 t_1 increments.

The 2D spin-exchange spectra give the information of the proximity due to the intermolecular hydrogen-bonding interaction between the phenolic hydroxyl group (OH) of PVPh and the C = O of PMMA, which is responsible for the miscibility of these PMMA/PVPh blends. As examples, spectra obtained at t_m = 2.0 ms are shown in Fig. 10(a-c) for Blend0, Blend120 (annealed at 120°C for 120 min) and Cast-film (made from solution), respectively. No intermolecular cross-peak between the OH and the C = O can be seen in Fig. 10(a) for pure powder blend, even the mixing time, t_m = 2 ms, which indicates an immiscible polymer blend. For the Blend120 annealed at 220°C for 120 min, Fig. 10(b) shows the cross-peak of the intermolecular hydrogen bonds when t_m = 2 ms, that is to say, the sample is miscible. Cast-film (shown in Fig. 5) gives a similar result with the Belnd120, while the signal intensity of cross-peak is strong enough even at a short mixing time of 0.5 ms (without being shown here). The results indicate that as the time of heat treatment is increased, the interchain diffusion of the polymers increases and the miscibility becomes easier. When the time is long enough, the heterogeneous powder blends become homogeneous like the miscible blend from solution. The spin-exchange results are in agreement with the above investigation results of ^{1}H spin-diffusion experiments.

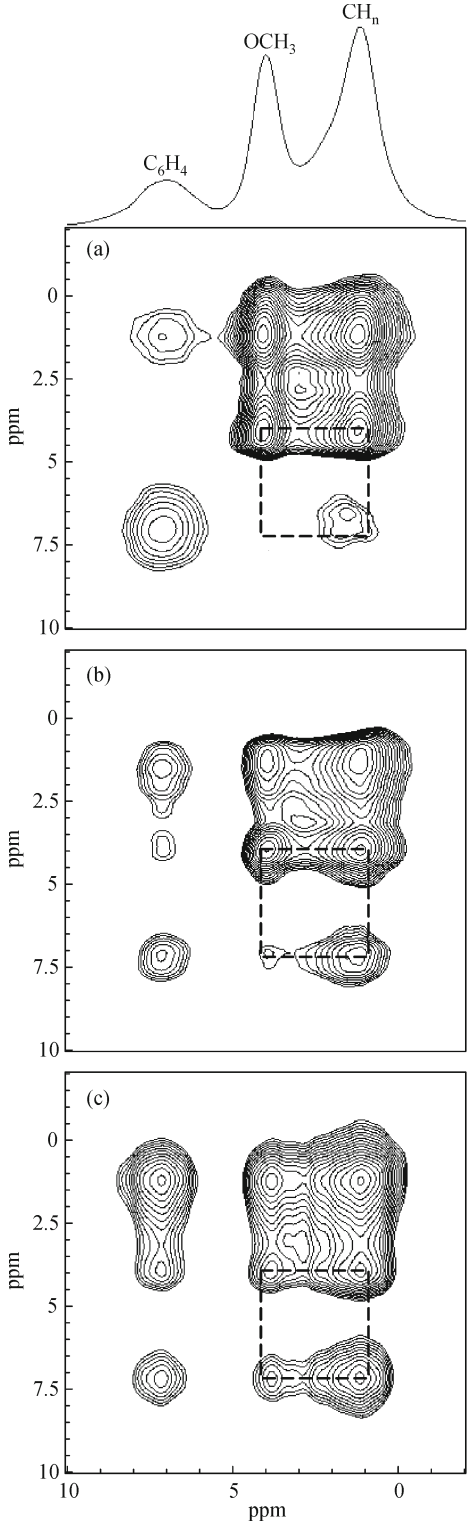

Figure 5 2D spin-exchange spectra of the PMMA/PVPh = 1/1 powder blends at mixing time (t_m) of 2 ms, for (a) Blend0 (powder blends), (b) Blend120 (annealed at 120°C for 120 min) and (c) Cast-film (made from solution). In the upper part the normal 1D spectrum is shown.

2.5 High-resolution ^{1}H-^{13}C HETCOR NMR experiments

Information about the molecular structures can be deduced from the strength of heteronuclear (^{1}H-^{13}C) dipolar interaction [120]. Heteronuclear correlation (HETCOR) NMR experiments can be applied to the analysis of ^{1}H-^{13}C and other heteronuclear correlations in a wide variety of crystalline and amorphous materials of practical interest [121]. It separated the dipolar interaction from the chemical shift interaction, resulting in 2D spectra with the chemical shift of each nucleus in one dimension correlated with its dipolar coupling to neighboring spins in the second dimension [122].The complete HETCOR experiment is illustrated in our previous work (as shown in Fig. 6) [119]. It has the classic four-part structure of preparation, evolution, mixing, and detection which is common to virtually all 2D NMR. It was acquired using 32 t_1 increments with 64 scans per increment, and 256 points in t_2. In this case, the spin system is prepared by a single pulse. During the evolution period, the protons are allowed to evolve in order to "label" them according to their chemical shifts under conditions of DUMBO-1 multiple-pulse for ^{1}H homonuclear decoupling. After the evolution period, a special mixing pulse sequence is applied to transfer polarization selectively from the protons to the carbon spins via the heteronuclear dipolar interaction. Finally, the ^{13}C FID is acquired during dipolar decoupling. During the entire experiment, the sample is rotated about the magic angle in order to suppress broadening due to chemical-shift anisotropy.

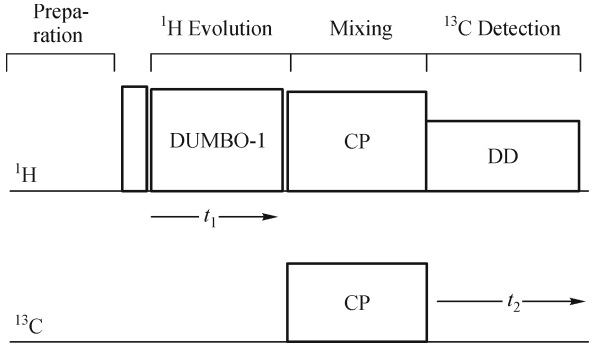

Figure 6 2D ^{1}H-^{13}C heteronuclear-correlation experiment (Homonulcear DUMBO-1 decoupling is applied during the ^{1}H evolution period.)

The 2D ^{1}H-^{13}C heteronuclear-correlation spectrum of PMMA/PVPh Cast film (polymer blends made from solution) is shown in Fig. 7, along with the ^{13}C chemical shifts and its molecular structure on the top. In this spectrum, the direct correlations are clearly resolved, and the long-range couplings of the nonprotonated carbon spins to their nearest proton

neighbors are also visible. A weak correlation circled with a red circle is observed connecting the hydroxyl protons (~7.5 ppm) and the carbonyl signal (at 178.3 ppm) from PMMA, indicating the formation of intermolecular hydrogen bonds in polymer blends. It is in good agreement with the above 2D ^{1}H-^{1}H spin-exchange experiments results, indicating that the Cast film samples made from solvent blend are intimately mixed on molecular scale.

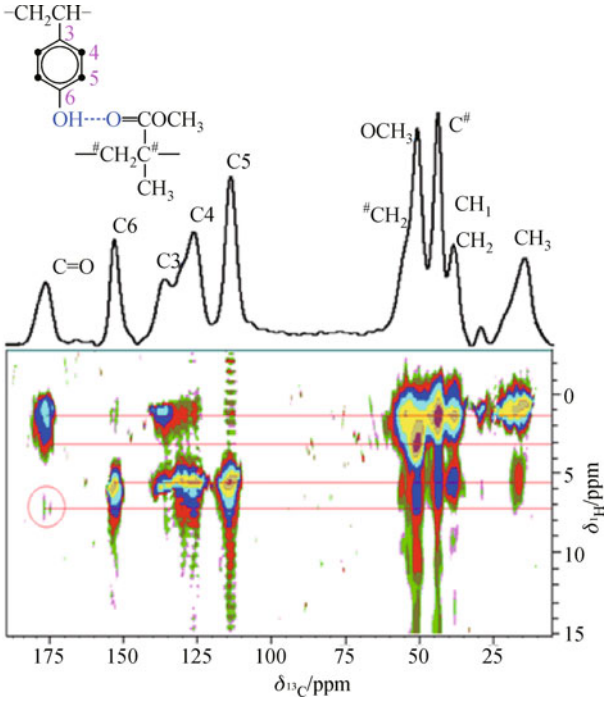

Figure 7 High-resolution 2D ^{1}H-^{13}C heteronuclear-correlation spectrum, 1D ^{13}C CP-MAS spectrum (top), and molecular structure of PMMA/PVPh blends made from solution. Correlations are evident both for directly bonded proton-carbon pairs and for couplings between nonprotonated carbons and their nearest neighbor protons (mixing time t_m = 10 μs).

2.6 Ab initio calculations

Ab initio calculations are now attainable and accurate enough to predict the structure and structure-property relationships for noncovalent interactions in complex hydrogen-bonded systems.

As it is well known, ^{1}H NMR chemical shifts (δs) are closely relevant to the understanding of the electronic structure in a molecule. An intra- or intermolecular hydrogen bonding will result in a decrease in diamagnetic shielding around the hydrogen nucleus. It makes the resonance of the proton concerned be shifted to a low field. This is referred to as the deshielding effect on the bridging hydrogen atom. Thus, ^{1}H δ-values can be used for identifying and characterizing hydrogen bonding. Ab initio density functional theory (DFT) calculation provided a new approach for investigating the NMR chemical shifts. Simulations using the software Gaussian (G03) with B3LYP as a level of theory, G-311 + FG as a basis set and exchange functions gauge including atomic orbital (GIAO) basis have been performed to calculate the CS shielding, parameters like χ and the asymmetry factor (η). For example, the principal value σ_{33} of ^{17}O chemical shift tensor moves up-field if the length of the hydrogen bond decreases [123]. It was elucidated that the relative arrangement of the hydrogen bonding groups in the polymer differs significantly from that of the monomer.

2.6.1 Gaussion quantum calculations on structure constants

To explore the effect of the molecular environment on the chemical-shift correlations between the ^{1}H and ^{13}C atoms of the polymer blends, the optimized equilibrium configurations with only one hydrogen bond by DFT/6-311G (2d, p) methods with O-H length of hydrogen bonds and the nearest distances between the methoxyl protons and the aromatic carbons in PMMA/PVPh blends are shown in Fig. 8. Wherein, the repeat units of the homopolymers are N = 5 with unfixed main chain dihedral angles and the molecular main-chain adopting random configuration. It can be seen that

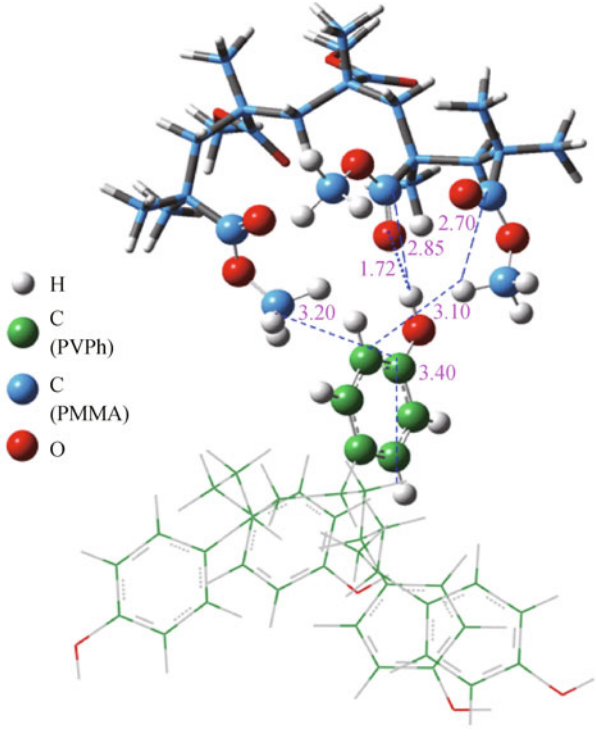

Figure 8 Hydrogen-bonded configuration between PMMA (N = 5) and PVPh monomer optimized by DFT methods. The hydrogen bond is drawn as thick blue lines for easy visualization. Selected interatomic distances (in Å) are indicated.

there are two side-chain OCH_3 groups of the random PMMA polymer, those nearest to and on both sides of the hydrogen bond (C = O…HO). Fig. 12 also displays that the distance between the OH proton and the C = O carbon is about 2.8 Å. Whereas the distances from OCH_3 protons to the nearest carbons atoms in the aromatic ring range from 3.0 to 3.2 Å, which is in the range of 2.7 Å (the distance from OCH_3 proton to the C = O carbon in the same side-chain) to 3.4 Å (from a carbon atom bound to OH group atom to the next nearest aromatic proton). The strength of the chemical-shift correlation peaks depends on the length of the interatomic distances, and therefore the correlation peaks of the neighboring groups, the OCH_3 protons with aromatic carbons, can be found in the ^{1}H-^{13}C HETCOR spectra (as shown in Fig. 7). We then calculated the NMR data at the B3LYP level using the gauge-including atomic orbital (GIAO) method. It approves the theoretical presumption that the special conformation of the intimate mixed blends is formed by the intermolecular hydrogen bond interaction. The calculations were also used to determine the hydrogen bonds in the polymer blends.

2.6.2 ^{13}C chemical shift anisotropy (CSA) tensors: A combination of density functional theory and SS NMR

The CSA patterns arise from the dependence of the chemical shift on molecular orientation in an applied static magnetic field. Therefore, they are sensitive to molecular motions and local molecular structure. CSA parameters can be extracted by a variety NMR techniques [124,132] and DFT calculations [133]. Recoupling of anisotropy information (RAI) was developed and applied here to *Bombyx mori* silk fibroin, a protein that forms heterogeneous semicrystalline fibers by Witter et al. [134,135]. Ernst' group calculated the ^{15}N CSA tensors of biomolecules, using DFT methods, to explore their dependence on the environment and on intramolecular dynamics, especially for the contribution of hydrogen bonding to CSA.

We used SPUPER NMR technique to obtain powder patterns of PMMA, PMMA/PVPh polymer blends [119]. The ^{13}C CSA patterns of the C = O in PMMA and the C = O…H-O hydrogen-bonded groups in PMMA/PVPh polymer blends from simulation by quantum chemical shift calculation and SPUER experimental spectra at room temperature are shown in Fig. 9. The corresponding theoretical calculation values (absolute values), ^{13}C anisotropic chemical shift tensor (δ_{11}, δ_{22} and δ_{33}) and isotropic chemical shift (δ_{iso}) of C = O group for the PMMA monomer and PVPh monomer blend with one hydrogen bond are listed in Table 2. Meanwhile, we calculated the corresponding chemical shift asymmetry (η) and chemical shift anisotropy (σ), which are defined as the following equation [136,137]. For $0 \leqslant \eta \leqslant 1$, when $|\delta_{11}-\delta_{iso}| \leqslant |\delta_{33}-\delta_{iso}|$, $\eta = (\delta_{22}-\delta_{11})/(\delta_{33}-\delta_{iso})$, and $\delta = \delta_{33}-(\delta_{11}+\delta_{22})/2$. While, when $|\delta_{11}-\delta_{iso}| \geqslant |\delta_{33}-\delta_{iso}|$, $\eta = (\delta_{22}-\delta_{33})/(\delta_{11}-\delta_{iso})$, and $\delta = \delta_{11}-(\delta_{22}+\delta_{33})/2$. As can be seen in Fig. 9(a), ^{13}C CSA powder patterns calculated from

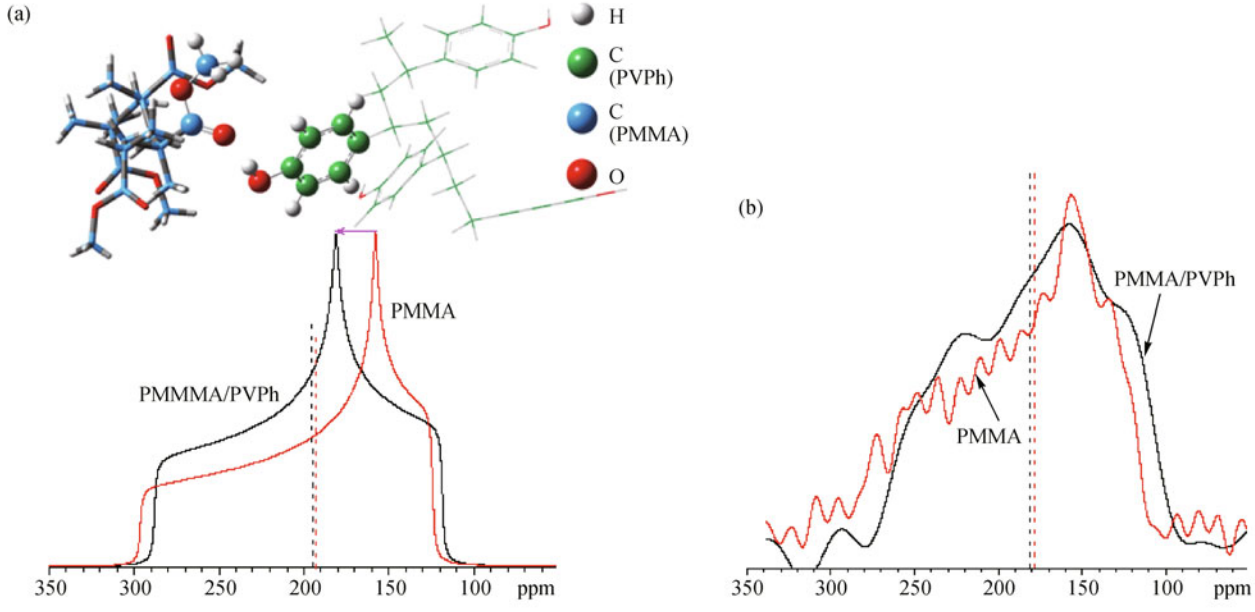

Figure 9 (a) Simulated powder patterns obtained with the average principal values given by ab initio chemical-shift calculation, for PMMA and PMMA/PVPh blend (its molecular structure on the top); (b) cross sections of C = O carbon powder spectra obtained from 2D super spectra of PMMA and PMMA/PVPh blends made from solution.

Table 2 Theoretical calculations on ^{13}C isotropic chemical-shift and principle values of CSA tensors (absolute values, ppm) for PMMA (denoted as PMMA1) and PMMA/PVPh monomer (denoted as PM1/PV1)

	σ_{iso}	σ_{11}	σ_{22}	σ_{33}	η	σ
PMMA1	−10.38	−113.86	24.53	58.17	0.325	−155.21
PM1/PV1	−12.79	−106.01	12.10	55.54	0.456	−139.78

$\delta_{ii} = \sigma_{ref} - \sigma_{ii}$, (i = 1, 2, 3), anisotropic chemical shift, σ_{ref} (= 182.46) is the shielding tensor of the reference compound, tetramethylsilane (TMS) for ^{13}C; $\delta_{iso} = 1/3(\delta_{11} + \delta_{22} + \delta_{33})$, isotropic chemical shift; η, chemical shift asymmetry; σ, chemical shift anisotropy

the principal values obtained from the ab inito calculations for PMMA and PMMA/PVPh models show features of an axially symmetric CSA tensor with the ^{13}C isotropic shift changes downfield near 2 ppm (as shown by a pink arrow). It is noted that after the hydrogen bond was formed, δ_{22} changed obviously about 50.7% and η increased by 40.3%, respectively. Fig. 9(b) shows the cross sections of C = O group powder spectra obtained from 2D SUPER spectra of PMMA and the PMMA/PVPh blends made from solutions. The changes of the CSA patterns and the ^{13}C isotropic shifts are found to be in good agreement with the simulation.

3 Misibility and phase behavior

Polymer blends are of major economic importance in the polymer industry. The physical and chemical properties of the materials depend not only on the nature of the constituent polymers but also on how intimately they are mixed [138]. Knowledge of the spatial proximity between the chains on different scales unveils information on compatibility, which has profound influence on the macroscopic properties of the final products. The compatibility in polymer blends has been received substantial attention in the past decades [139–141]. Intermolecular-specific interactions (e.g., hydrogen bonding, dipole-dipole interaction, or ionic interaction) are increasingly used for compatible polymer blends. This approach is especially versatile because the degree of blend miscibility should be controlled directly by the chemical structure, composition, strength of the interaction, and the concentration of functional groups used to induce phase mixing. Today, it is well-established that inter-associated hydrogen bonding between the components promotes the compatibility and the miscibility of polymer blends as well [142]. In fact, nowadays, the introduction of hydrogen bonds is a routine and effective strategy to achieve the compatibility and modify the properties of the blends [138–141].

During the past two decades, a lot of work on determining miscibility in polymer blends with hydrogen bonding based on NMR measurements have been reported [143], mainly including relaxation time (T_1, T_2, $T_{1\rho}$) [144], 2D WISE, spin diffusion, and so on. Here, a new chemical-shift filtered high-resolution NMR pulse sequence based on a recently developed continuous phase modulation technique is proposed, which is used to clearly elucidate the miscrostructure and miscibility by being simultaneously combined with the spin-diffusion experiments.

^{1}H chemical-shift-filter spin diffusion new methods. The nuclear magnetization of specific protons in one polymer phase can be selected either by exploiting differences in the molecular mobility or in the chemical composition of the constituents. For PMMA/PVPh rigid/rigid polymer blends system, proton spin-diffusion experiments (Fig. 10) based on the differences in proton chemical shifts under CRAMPS conditions were used [119]. To select a specific proton-magnetization component, one has to suppress at least two other components using ^{1}H CRAMPS filter [145]. By properly adjusting the proton carrier frequency, the duration of the multipulse irradiation, and the preparation pulse, one can indeed select the proton magnetization of the phenyl rings in PVPh, or of the methoxy group in PMMA.

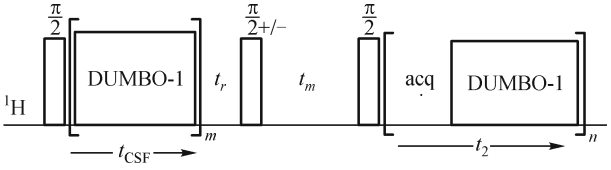

Figure 10 Pulse sequence of ^{1}H spin diffusion CRAMPS based on the chemical shift filter (CSF)

Fig. 11 shows the ^{1}H high-resolution CRAMPS spectra after CSF selection of methoxy protons in PMMA during different mixing time (t_m), from 0.0002 to 10 ms for the PMMA/PVPh polymer blends: Blend0 (powder blends), Blend120 (annealed at 120°C for 120 min) and Cast film (made from solution). These chemical shift filter (CSF) spin diffusion experiments will provide information about the domain sizes of the PMMA/PVPh blends. For Blend0 (Fig. 11(a)), the increase in the signal intensity in the spectral region of aliphatic protons (δ_H = 1–2 ppm) reflects spin diffusion from the methoxy protons to the main chain protons of PMMA, while hardly any proton magnetization reaches the aromatic proton in PVPh structures (δ = 7–8 ppm), even after mixing times as long as 50 ms (without being shown here). For Blend120 (Fig. 11(b)), the equilibration of the proton-

magnetization distribution occurs on a time scale of 10 ms. For the Cast film (Fig. 11(c)), the intensity of the aromatic proton signal of PVPh is relatively large compared with that of the Blend120 in shorter mixing times. This indicates that spin diffusions occurring fairly fast give evidence of intimate mixing for PMMA and PVPh.

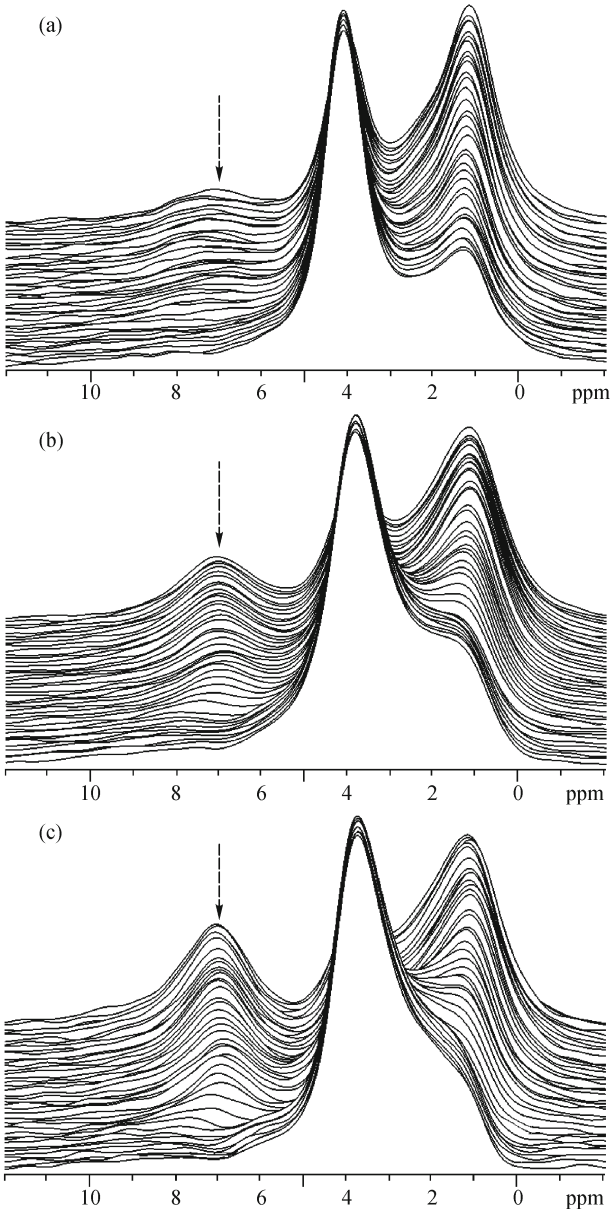

Figure 11 Spectra of ^{1}H CSF spin-diffusion of PMMA/PVPh samples for (a) Blend0 (b) Blend120 and (c) Cast film. Corresponding spin diffusion times are from 0.0002–10 ms.

4 Molecular dynamics

Molecular dynamics on different length and time scales dominate the mechanical properties of solid polymers [146]. SS NMR is a very suitable technique for the study of the structure and dynamics of polymers and biomacromolecules at a molecular level [147]. Traditionally, line shape analysis [41,57,148–151], or relaxation time measurements of protons or deuterons [152–155] can be used for this purpose.

Fast local motions fall in the domain of NMR methods based on longitudinal spin relaxation of suitable nuclei such as protons or carbon-13, where the study of the relaxation dispersion over a large frequency range for the former via field-cycling methods [156,157] or the chemical resolution of the latter [158] are the basis of the most powerful strategies, and do not even require isotopic labeling. Kevin S. Jack and Andrew K. Whittaker [154] investigated the changes in molecular motions in blends of PEO/PVPh using measurements of solid-state $T_{1\rho}$ relaxation times. A short $T_{1\rho}$ has been observed for protonated aromatic carbons, and assigned to phenyl rings undergoing large-angle oscillatory motion. The effects of blending, and temperature on the proportion of rings undergoing oscillatory motion are analyzed.

NMR spectra are dominated by the nuclear shielding tensor (anisotropic chemical shift), which can be analyzed to yield quantitative information about rotational motions [159]. In polymer science people are particularly interested in the mobility of macromolecular chains, the basic ones being aliphatic. Unfortunately, the anisotropy of the nuclear shielding is generally small for both ^{1}H and ^{13}C in aliphatic groups [160] and, moreover, the shielding tensors are not axially symmetric. However, ^{2}H NMR techniques allow us to monitor rotational motions over a wide range of characteristic frequencies, including the fast (200–10^{7} kHz), intermediate (15–150 kHz), and slow (0.4–10 kHz) motions. The chain mobility of a series of hydrogen-bonded polymer complexes and multilayers were compared by variable temperature wide-line deuterium NMR spectroscopy by Reven's group [161]. Wherein, the series of water saturated complexes took form from deuterium labeled poly (methacrylic acid), PMAA-d3 and a range of hydrogen accepting polymers that have been used to produce pH responsive multilayer films and capsules. The polymers examined are listed, along with some thermal parameters, in Table 3.

^{2}H NMR line shape analysis. The ^{2}H NMR spectra of the series of PMAA complexes saturated with acidic water over a

Table 3 Polymer properties[161].

Polymer	T_g/°C	Solution critical temperature
PMAA	228	
PVPon	177	
PVCL	145	31°C–37°C LCST
PEO	−55	
PVME	−31	35°C LCST
PAAM	165	20°C–25°C UCST for the PAAm/PAA network
chitosan	203	

temperature range of 21°C–70°C are presented in Fig. 12. The onset of chain mobility with increasing temperature is indicated by the averaging of the Pake pattern to an isotropic peak. In the case of the weak PEO (low-T_g, mobile polymer)/PMAA complex, a significant isotropic component is present even before heating, and the broad component vanishes upon warming just above room temperature. The PAAM (a high Tg, thermoresponsive polymer)/PMAA complexes display an isotropic component with moderate heating but, unlike the PEO complex, retain broad components at the highest temperatures examined. The chitosan-PMAA polyelectrolyte complex displays an onset of motion with frequencies in the intermediate rather than fast regime as signaled by the gradual attenuation of the Pake pattern intensity. Despite the polymers that form the strongest complexes with PVPon, the PMAA chain motion remains restricted with no significant change in the ^{2}H Pake pattern line shapes with heating. Even the thermoresponsive properties of PVME and PVCL have little or no effect on the PMAA chain dynamics as expected since complexes of polymers with LCSTs are known to stabilize with heating. It is concluded that through the selection of appropriate partner polymers, the chain mobility and related properties of PMAA-based complex can be continuously tuned, ranging from highly mobile for hydrophilic polymers (PEO or PAAM) where fast isotropic motion is observed to dominate, to a thermally stable glassy state for partner polymers with significant hydrophobic character (PVPon or PVCL).

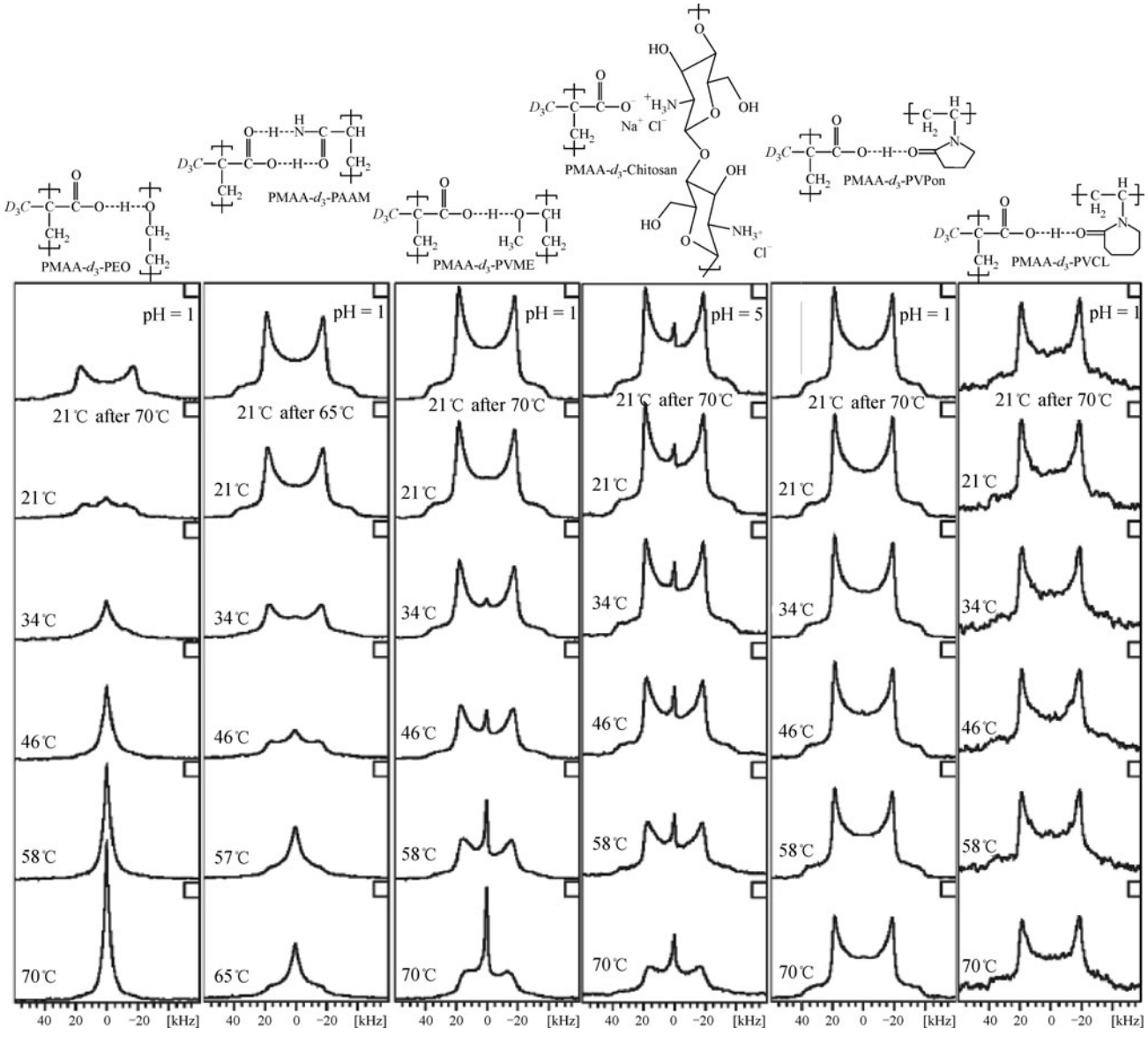

Figure 12 Variable temperature ^{2}H NMR of ~40 wt% PMAA-d_3 complexes saturated with acidic deuterium depleted water, with the exception of the chitosan complex which was saturated with untreated deuterium depleted water [161].

Proton multiple-quantum NMR method. Purely geometric confinement of small molecules and polymers on the nanometer scale has attracted much attention recently, mainly because of the unusual and sometimes counterintuitive changes which occur in the molecular conformation, the dynamics, and the glass transition. Understanding the surface-induced phenomena is of paramount importance for the proper design of new materials that are structured on the nanometer level, such as polymers filled with nano-sized fillers or thin films for sensor applications.

The proton multiple-quantum NMR method is often employed to stabilize multicomponent polymer systems and to achieve favorable wetting conditions or good dispersion, and therefore increase the mechanical properties such as superior elongation property [162], flexible modulus and thermal stability [163,164]. What has particular commercial relevance is the modification of inorganic filler particles for reinforcement or viscosity control of elastomers and polymer melts. Blumich and coworkers [165] studied the dynamics of ultra thin flexible polymer, poly-dimethylsiloxane (PDMS) films (up to about four monomer thick) adsorbed on porous substrates by employing ^{1}H DQ NMR techniques. Fig. 13 shows DQ build-up curves for a low temperature (221 K), where two distinct maxima are observed and can be attributed to a rather rigid surface layer and another more mobile domain. This method can also be applied to study interphase interaction of the organic/inorganic, such as poly(N-isopropylacrylamide (PNIPA), polyurethane foam/clay networks.

Usually, a ^{1}H-^{1}H DQ signal can be observed when the two protons have a maximum distance of ~350 pm. The 2D DQ MAS NMR correlation spectra can serve as a method to determine the local packing environment of amorphous materials. Traer and Goward [105] used DQ MAS NMR to determine the proton dynamics. A combination of solid-state ^{1}H NMR techniques, namely MAS, CRAMPS, and DQ MAS spectroscopy, was used to investigate the hydrogen bonding properties of a range of alkyl-substitued benzoxazine dimmers by Schnell et al. [167].

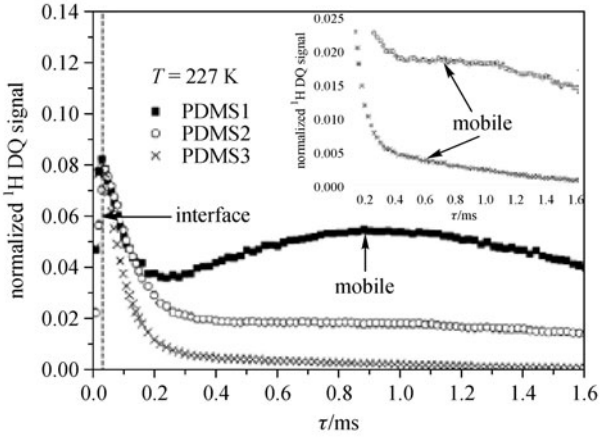

Figure 13 500 MHz proton DQ build-up curves for short PDMS grafts on silica, measured with the two-pulse segment. The surface coverage, thus the average length of PDMS dangling ends and loops decreases from PDMS1 to PDMS3. Note that "normalized" here refers only to an intensity scale where the unity corresponds to the full sample magnetization. Figure reprinted with permission from Ref. [103]

PISEMA experiment. Although a variety of SS NMR techniques have been successfully used to study the hydrogen bonding interactions in polymers and other organic solids [94,145,168–170], few NMR studies have been reported so far to elucidate the local molecular dynamics dependence on hydrogen bonding in polymer blend [171]. To examine the influence of strong intermolecular hydrogen bonding on the local molecular dynamics of polymer blends, we studied miscible PVPh/PMMA mixtures with different compositions using ^{13}C-^{1}H PISEMA method [119].

The polarization inversion spin exchange at the magic angle (PISEMA) experiment [172] is a widely used technique for measurements of heteronuclear dipolar couplings in membrane-bound peptides and proteins [173,174], as well as liquid-crystalline samples [175]. Fig. 14 shows the pulse sequence of amplitude modulated PISEMA [176] spectrum of our polymer blends. After standard ^{1}H-^{13}C CP, the ^{1}H magnetization is aligned at the magic angle to the static magnetic field by means of a ^{1}H 35° pulse. It is subsequently spin-locked by off-resonance flip-flop LG irradiation and matched by a phase-alternated ^{13}C RF field. The heteronuclear dipolar couplings are monitored through the oscillations resulting from coherent polarization transfer between ^{1}H and ^{13}C spins during t_1. Under MAS with a spinning frequency ω_r, the Hartmann-Hahn (HH) matching condition must be satisfied for efficient spin exchange, $\omega_{eff,H} - \omega_{1,C} = n\omega_r$, $n = \pm 1$, where $\omega_{eff,H} = (3/2)^{1/2}\gamma_H B_{1H}$ and $\omega_{1,C} = \gamma_{1C}B_{1C}$. The spinal-64 pulse sequence is used during the acquisition period, t_2.

The influence of the local chain mobility on the cooperative chain motion between the CH_3 of PMMA and the aromatic

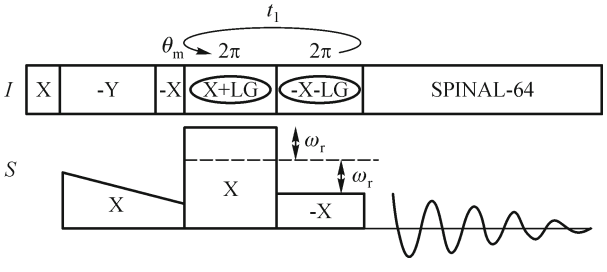

Figure 14 PISEMA pulse sequence for molecular dynamic study

proton of PVPh can be studied by PISEMA high resolution solid state SS NMR techniques. Fig. 15(a) shows the 2D ^{1}H-^{13}C experimental dipolar spectrum using PISEMA method for PMMA/PVPh polymer blend made by mixing solutions, with the ^{13}C spectrum and its corresponding molecular structures shown on the top. The cross section of aromatic carbon (C5) at 116.0 ppm have two splits for both the two blends, the Blend 120 (powder blend annealed for 120 min) plotted as black line and the Cast film (made from solution) plotted as blue line (Fig. 15(b)) at room temperature. The splitting width ($\Delta\nu$) depends on the intensity of ^{1}H-^{13}C dipolar coupling, especially for the strong interactions, and thus indicates the mobility of molecular motions. The wide splitting denotes the rigid aromatic group, while the narrower peak results in the wobbling motion. Due to the existing plentiful hydrogen bonds in the miscible Cast film, the motivation amplitude of aromatic proton in PVPh can be increased greatly by the 180° flipping of methyl proton in PMMA [144,177]. Therefore, it can be seen that the intensity of the narrower peak ($\Delta\nu$ = 7.8 kHz) in the Cast film is stronger (Fig. 15(b)).

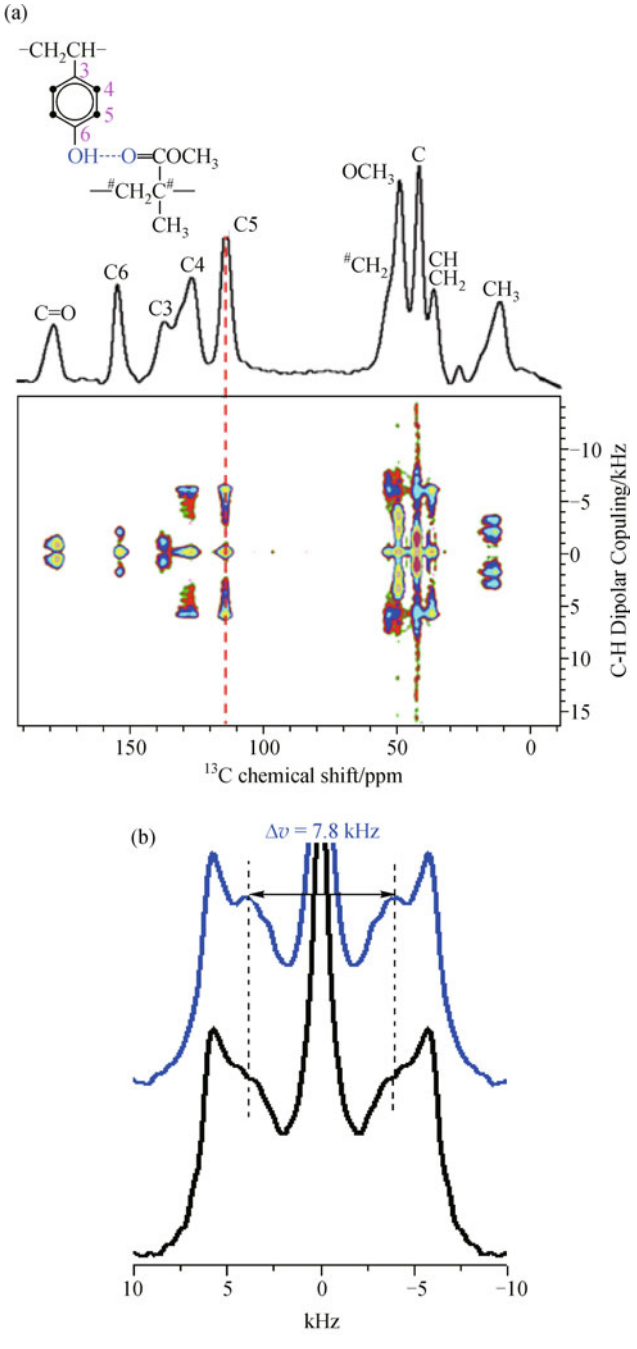

Figure 15 (a) 2D PISEMA spectrum of PMMA/PVPh polymer blends made from Cast film. Cross sections of (b) the aromatic proton (δ = 116.0 ppm) for Blend120 (bottom) and Cast film (top) at room temperature.

5 Conclusions

We hope that we have provided useful information in this article about how solid-state NMR affords valuable and detailed insight into the miscibility, phase behavior and dynamics of a wide range of hydrogen-bonded polymer materials. This account outlined the recent progress in this field with a focus on latest contributions. The use of a multinuclear and multi-quantum approach in the solid-state NMR investigation allows us to obtain information, at the local level, opening new perspectives in the prediction and design of multiphase polymer systems. Hydrogen bonds, phase behavior, and dynamics of molecular segments can be investigated in great details, in most cases without the need for special sample preparation. This implies new possible applications in many important fields such as drug delivery, sensor probes, tissue engineering.

Acknowledgements This work was financially supported by Teaching group of Tianjin Polytechnic University (2010-C-02) and the National Science Fund for Distinguished Young Scholars (No. 20825416). We thank Dr. Que Gi of Nanjing University for a carefully proofreading of the manuscript.

References

1. Cooper, S. L.; Estes, G. M., *Multiphase polymers*. **1979**, 176
2. Jiang, M.; Li, M.; Xiang, M.; Zhou, H., *Adv. Polym. Sci*. **1999**, *146*, 121–196
3. Scheiner, S., Hydrogen Bonding; Oxford University Press: New York, **1997**.
4. Jeffrey, G. A., An introduction to Hydrogen Bond; Oxford University Press: New York, **1997**.
5. Scanlon, S.; Aggeli, A., *Nano Today* **2008**, *3*, 22–30
6. Kuo, S. W.; Hsu, C. H., *Polym. Int*. **2010**, *59*, 998–1005

7. Schmidt-Rohr, K.; Spiess, H. W., Multidimensional solid-state NMR and polymers. 1st ed., Academic Press, London, **1994**
8. deDios, A. C.; Oldfield, E., *J. Am. Chem. Phys*. **1994**, *116*, 5307–5314
9. Duffy, D. M.; Rodger, P. M., *J. Am. Chem. Soc*. **2002**, *124*, 5206–5212
10. Cui, L.; Zhao, Y., *Chem. Mater*. **2004**, *16*, 2076–2082
11. Quinn, J. F.; Caruso, F., *Langmuir* **2004**, *20*, 20–22 (PAA-LBL)
12. Khutoryanskiy, V. V.; Dubolazov, A. V.; Nurkeeva, Z. S.; Mun, G. A., *Langmuir* **2004**, *20*, 3785–3790
13. Peng, C. C.; Abetz, V., *Macromolecules* **2005**, *38*, 5575–5580
14. Lutkenhaus, J. L.; Hrabak, K. D.; McEnnis, K.; Hammond, P. T., *J. Am. Chem. Soc*. **2005**, *127*, 17228–17234
15. Kuo, S-W.; Chen, C. J.; *Macromolecules* **2011**, on line
16. Hu, J. Z.; Solum, M. S.; Taylor, C. M. V.; Pugmire, R. J.; Grant, D. M., *Energy Fuels* **2001**, 15, 14–22bb
17. Hartzell, C. J.; Whitfeld, M.; Oas, T. G.; Drobny, G. P., *J. Am. Chem. Soc.* **1987**, *109*, 5966–5969
18. Havlin, R. H.; Le, H.; Laws, D. D.; deDios, A. C.; Oldfield, E., *J. Am. Chem. Soc.* **1997**, *119*, 11951–11958
19. Perez, S., In Water and Biological Macromolecules; Westthof, E., Ed.; The Macmillan Press Ltd.: Houndmills, Basingstoke, London, **1993**; Chapter 10, 295–320
20. McBrierty, V. J.; Quinn, F. X.; Keely, C.; Wilson, A. C.; Friends, G. D., *Macromolecules* **1992**, *25*, 4281–4284
21. Calucci, L.; Forte, C.; Ranucci, E., *Biomacromolecules* **2007**, *8*, 2936–2942
22. Schmidt-Rohr, K.; Clauss, J.; Blumich, B.; Spiess, H. W., *Magn. Reson. Chem*. **1990**, *28*, S3–S9
23. Spiess, H. W., *Polymer* (Academic, San Diego, 1994).
24. Hirschinger, J.; Miura, H.; Gardner, K. H.; English, A. D., *Macromolecules* **1990**, *23*, 2153–2169
25. Miura, H.; Hirschinger, J.; English, A. D., *Macromolecules* **1990**, *23*, 2169–2182
26. Cai, W. Z.; Schimidt-Rohr, K.; Egger, N.; Gerharz, B.; Spiess, H. W., *Polymer (Guildf.)* **1993**, *34*, 267–275
27. Saalwachter, K., *Prog. Nucl. Magn. Reson. Spectrosc*. **2007**, *51*, 1–35
28. Aliev, A. E.Harris. K. D. M., *Struct. Bond*. **2004**, *108*, 1–53
29. Goward, G. R.; Sebastiani, D.; Schnell, I.; Spiess, H. W.; Kim, H. D.; Ishida, H., *J. Am. Chem. Soc*. **2003**, *125*, 5792–5800
30. Yates, J. R.; Pham, T. N.; Pickard, C. J.; Mauri, F.; Amado, A. M.; Gil, A. M.; Brown, S. P., *J. Am. Chem. Soc*. **2005**, *127*, 10216–10220
31. Gervais, C.; Dupree, R.; Pike, K. J.; Bonhomme, C.; Profeta, M.; Pickard, C. J.; Mauri, F., *J. Phys. Chem. A* **2005**, *109*, 6960–6969
32. Schmidt, J.; Sebastiani, D. *J. Chem. Phys*. **2005**, *123*, 074501;
33. Schmidt, J.; Hoffmann, A.; Spiess, H. W.; Sebastiani, D., *J. Phys. Chem. B* **2006**, *110*, 3204–3210
34. Schulz-Dobrick, M.; Metzroth, T.; Spiess, H. W.; Gauss, J.; Schnell, I., *ChemPhysChem* **2005**, *6*, 315–327
35. Uldry, A. C.; Griffin, J. M.; Yates, J. R.; Pérez-Torralba, M.; María, M. D.; Webber, A. L.; Beaumont, M. L.; Samoson, A.; Claramunt, R. M.; Pickard, C. J.; Brown, S. P., *J. Am. Chem. Soc*. **2008**, *130*, 945–954
36. Williams, J.; McDermott, A., *J. Phys. Chem*. **1993**, *97*, 12393–12396
37. deDios, A. C.; Oldfield, E., *J. Am. Chem. Phys*. **1994**, *116*, 5307–5314
38. Takegoshi, K., *Annu. Rep. NMR Spectrosc*. **1995**, *30*, 97–126
39. Asano, A.; Takegoshi, K., Solid State NMR of Polymers, Chapter 10, I. Ando and T. Asakura, eds., Elsevier, Netherlands, **1998**, *35*, 1–414
40. Fyfe, C. A., in Solid State NMR for Chemists, C. F. C. Press, Guelph, **1983**.
41. Schmidt-Rohr, K.; Clauss, J.; Spiess, H. W., *Macromolecules* **1992**, *25*, 3273–3277
42. Sun, P. C.; Dang, Q. Q.; Li, B. H.; Chen, T.; Wang, Y.; Lin, H.; Jin, Q.; Ding, D.; Shi, A.C., *Macromolecules* **2005**, *38*, 5654–5667
43. Saito, S.; Moteki, Y., *Macromolecules* **1990**, *23*, 3256–3260
44. Tycko, R., How does NMR probe molecular dynamics? In Nuclear Magnetic Resonance Probes of Molecular Dynamics; Tycko R.,, Ed.; Kluwer Academic Publishers: New York, **1994**
45. Hodgkinson, P.; Crystallography, N. M. R.; Harris, R. K.; Wasylishen, R. E.; Duer, M. J., eds., EMR Handbooks Wiley: New York, **2009**; Chapter Intramolecular motion in crystalline organic solids
46. Schmidt-Rohr, K., Spiess, H. W., Multidimensional Solid-State NMR and Polymers; Academic Press: New York, **1994**.
47. Tycko, R.; Dabbagh, G.; Mirau, P. A., *J. Magn. Reson*. **1989**, *85*, 265–274
48. Schaefer, J.; Sefcik, M. D.; Stejskal, E. O.; McKay, R. A., *Macromolecules* **1984**, *17*, 1118–1124
49. Spiess, H. W., Colloid & Polymer Sci., *Polymer Science* **1983**, *261*, 193–209
50. Schmidt-Rohr, K.; Clauss, J.; Spiess, H. W., *Macromolecules* **1992**, *25*, 3273–3277
51. Paris, M.; Bizot, H.; Emery, J.; Buzaré, J. Y.; Buléon, A., *Int. J. Biol. Macromol*. **2001**, *29*, 137–143
52. Mulder, F. M.; Jansen, B. J. P.; Lemstra, P. J.; Meijer, H. E. H.; de Groot, H. J., *Macromolecules* **2000**, *33*, 457–460
53. Yan, B.; Stark, R. E., *Macromolecules* **1998**, *31*, 2600–2605
54. Munowitz, M.; Aue, W. P.; Griffin, R. G., *J. Chem. Phys*. **1982**, *77*, 1686–1689
55. Van Rossum, B. J.; de Groot, C. P.; Ladizhansky, V.; Vega, S.; de Groot, H. J. M., *J. Am. Chem. Soc*. **2000**, *122*, 3465–3472
56. Schaefer, J.; Stejskal, E. O.; Perchak, D.; Skolnick, J.; Yaris, R., *Macromolecules* **1985**, *18*, 368–373
57. Zhang, Y.; Hong, M.; Yao, X.; Jakes, K.; Hutter, D., *J. Phys. Chem. B* **2002**, *106*, 7355–7364
58. Marassi, F. M.; Ma, C.; Gesell, J. J.; Opella, S. J., *J. Magn. Reson*. **2000**, *144*, 156–161
59. Wang, J.; Kim, S.; Kovacs, F.; Cross, T. A., *Protein Sci*. **2001**, *10*, 2241–2250
60. Mehring, M.; Waugh, J. S., *Phys. Rev. B* **1972**, *5*, 3459–3471
61. Dvinskikh, S. V.; Zimmermann, H.; Maliniak, A.; Sandström,

D., *J. Magn. Reson*. **2003**, *164*, 165–170
62. Aronson, C. L.; Beloskur, D.; Frampton, I. S.; McKie, J.; Burland, B., *Polym. Bull*. **2005**, *53*, 413–424
63. Jeffrey, G. A.; Saenger, W., Hydrogen bonding in biological structure, Berlin: Springer; 1991.
64. Fortier-McGill, B.; Toader, V.; Reven, L. *Macromolecules*, **2011**, *44*, 2755–2765
65. McQuade, D. T.; McKay, S. L.; Powell, D. R.; Gellman, S. H., *J. Am. Chem. Soc*. **1997**, *119*, 8528–8532
66. Dong, J.; Ozaki, Y.; *Macromolecules*. **1997**, *30*, 286–292
67. Li, D.; Brisson, J.; *Polymer (Guildf.)* **1999**, *39*, 793–800
68. Stuart, B. H., *Polym. Bull*. **1994**, *33*, 681–686
69. Taylor, L. S.; Langkilde, F. W.; Zografi, G., *J. Pharm. Sci*. **2001**, *90*, 888–901
70. Hill, D. J. T.; Whittaker, A. K.; Wong, K. W., *Macromolecules* **1999**, *32*, 5285–5891
71. Hietala, S.; Maunu, S. L.; Sundholm, F.; Lehtinen, T.; Sundholm, G., *J. Polym. Sci., B, Polym. Phys*. **1999**, *37*, 2893–2900
72. Feindel, K. W.; Bergens, S. H.; Wasylishen, R. E., *ChemPhysChem* **2006**, *7*, 67–75
73. Nishiyama, Y.; Langan, P.; Chanzy, H, *J. Am. Chem. Soc.* **2002**, *124*, 9074–9082
74. Nishiyama,Y.; Sugiyama, J.; Chanzy, H., Langan, P., *J. Am. Chem. Soc*. **2003**, *125*, 14300–14306
75. Dunkers, J.; Zarate, E. A.; Ishida, H., *J. Phys. Chem*. **1996**, *100*, 13514–13520
76. Witter, R.; Sternberg, U.; Hesse, S.; Kondo, T.; Koch, F. T.; Ulrich, A. S., *Macromolecules* **2006**, *39*, 6125–6132
77. Steiner, T., *Angew. Chem. Int. Ed*. **2002**, *41*, 48–76
78. Asakawa, N., Kameda, T.; Kuroki, S.; Kurosu, H.; Ando, S.; Ando, I.; Shoji, A., *Annual Reports on NMR Spectroscopy* **1998**, *35*, 55–137
79. Colemm, M. M.; Painter, P. C., *Prog. Polym. Sci*. **1995**, *20*, 1–59
80. He, Y.; Zhu, B.; Inoue, Y., *Prog. Polym. Sci*. **2004**, *29*, 1021–1051
81. Kuo, S. W.; *J. Polym. Res*. **2008**, *15*, 459–486
82. Chierotti, M. R.; Gobetto, R., *Chem. Commun. (Camb.)* **2008**, *14*, 1621–1634
83. Feindel, K. W.; Bergens, S. H.; Wasylishen, R. E., *ChemPhysChem* **2006**, *7*, 67–75
84. Hietala, S.; Maunu, S. L.; Sundholm, F.; Lehtinen, T.; Sundholm, G., *J. Polym. Sci., B, Polym. Phys*. **1999**, *37*, 2893–2900
85. Takigami, S.; Kimura, T.; Nakamura, Y., *Polymer (Guildf.)* **1993**, *34*, 604–609
86. Higuchi, A.; Lijima, T., *Polymer (Guildf.)* **1985**, *26*, 1207–1211
87. Bronnimann, C. E.; Zeigler, R. C.; Maciel, G. E., *J. Am. Chem. Soc*. **1988**, *110*, 2023–2026
88. Liu, C. C.; Maciel, G. E., *J. Am. Chem. Soc*. **1996**, *118*, 5103–5119
89. Samoson, A.; Tuherm, T.; Gan, Z., *Solid State Nucl. Magn. Reson*. **2001**, *20*, 130–136
90. Gerstein, B. C.; Pembleton, R. G.; Wilson, R. C.; Ryan, L. M., *J. Chem. Phys*. **1977**, *66*, 361–373
91. Burum, D. P.; Rhim, W. K., *J. Chem. Phys*. **1979**, *71*, 944–950
92. Bronnimann, C. E.; Hawkins, B. L.; Zhang, M.; Maciel, G. E., *Anal. Chem*. **1988**, *60*, 1743–1750
93. Elena, B.; de Paepe, G.; Emsley, L., *Chem. Phys. Lett*. **2004**, *398*, 532–538
94. Li, B.; Xu, L.; Wu, Q.; Chen, T.; Sun, P.; Jin, Q.; Ding, D.; Wang, X.; Xue, G.; Shi, A. C., *Macromolecules* **2007**, *40*, 5776–5786
95. Schnell, I.; Spiess, H. W., *J. Magn. Reson*. **2001**, *151*, 153–227
96. Brown, S. P.; Spiess, H. W., *Chem. Rev*. **2001**, *101*, 4125–4156
97. Pawsey, S.; McCormick, M.; De Paul, S.; Graf, R.; Lee, Y. S.; Reven, L.; Spiess, H. W., *J. Am. Chem. Soc*. **2003**, *125*, 4174–4184
98. Ba, Y.; Ripmesster, J. A., *J. Chem. Phys*. **1998**, *108*, 8589–8594
99. Saalwachter, K., *Prog. Nucl. Magn. Reson. Spectrosc*. **2007**, *51*, 1–35
100. Sommer, W.; Gottwald, J.; Demco, D. E.; Spiess, H. W., *J. Magn. Reson. A* **1995**, *113*, 131–134
101. Feike, M.; Demco, D. E.; Graf, R.; Gottwald, J.; Hafner, S.; Spiess, H. W., *J. Magn. Reson. A* **1996**, *122*, 214–221
102. Graf, R.; Demco, D. E.; Hafner, S.; Spiess, H. W., *Solid State Nucl. Magn. Reson*. **1998**, *12*, 139–152
103. Schnell, I.; Langer, B.; Söntjens, S. H. M.; van Genderen, M. H. P.; Sijbesma, R. P.; Spiess, H. W., *J. Magn. Reson*. **2001**, *150*, 57–70
104. Schnell, I.; Langer, B.; Sontjens, S. H. M.; Sijbesma, R. P.; van Genderen, M. H. P.; Spiess, H. W., *Phys. Chem. Chem. Phys*. **2002**, *4*, 3750–3758
105. Armstrong, G.; Alonso, B.; Massiot, D.; Buggy, M., *Magn. Reson. Chem*. **2005**, *43*, 405–410
106. Bonhomme, C.; Hartmeyer, G.; Babonneau, F.; Man, M. W. C.; Arrachart, G.; Carcal, C.; Moreau, J.; Alonso, B., *Mater. Res. Soc. Symp. Proc*. **2007**, *1008*, T02–09
107. Arrachart, G.; Carcel, C.; Moreau, J. J. E.; Hartmeyer, G.; Alonso, B.; Massiot, D.; Creff, G.; Bantignies, J. L.; Dieudonne, P.; Man, M. W. C.; Althoff, G.; Babonneau, F.; Bonhomme, C., *J. Mater. Chem*. **2008**, *18*, 392–399
108. Mafra, L.; Gomes, J. R. B.; Trébosc, J.; Rocha, J.; Amoureux, J. P., *J. Magn. Reson*. **2009**, *196*, 88–91
109. Gerothanassis, I. P., *Prog. Nucl. Magn. Reson. Spectrosc.* **2010**, *56*, 95–197.
110. Lemaître, V.; Smith, M. E.; Watts, A., *Solid State Nucl. Magn. Reson.* **2004**, *26*, 215–235
111. Suresh, C. G.; Vijayan, M., *Int. J. Pept. Protein Res*. **1983**, *22*, 129–143
112. Kuroki, S.; Takahashi, A.; Ando, I.; Shoji, A.; Ozaki, T., *J. Mol. Struct*. **1994**, *323*, 197–208
113. Yamauchi, K.; Kuroki, S.; Ando, I.; Ozaki, T.; Shoji, A., *Chem. Phys. Lett*. **1999**, *302*, 331–336
114. Mirau, P. A.; Tanake, H.; Bovey, F. A., *Macromolecules* **1988**, *21*, 2929–2933

115. Mirau, P. A.; Heffner, S. A.; Koegler, G. K.; Bovey, F., *Polym. Int*. **1991**, *26*, 29–34
116. Macura, S.; Ernst, R. R., *Mol. Phvs*. **1980**, *41*, 95–117
117. Jeener, J.; Meier, B. H.; Bachmann, P.; Ernst, R. R., *J. Chem. Phys*. **1979**, *71*, 4546–4553
118. Caravatti, P.; Neuenschwander, P.; Ernst, R. R., *Macromolecules* **1985**, *18*, 119–122
119. Fu, W. G.; Sun, P. C.; Zhang, R. C.; Lin, H.; Li, B. H.; Jin, Q. H.; Ding, D. T., *Macromolecules*, to be submitted.
120. van Rossum, B. J.; de Groot, C. P.; Ladizhansky, V.; Vega, S.; de Groot, H. J. M., *J. Am. Chem. Soc*. **2000**, *122*, 3456–3472
121. White, J. L.; Mirau, P. A., *Macromolecules* **1994**, *27*, 1648–1650
122. Bronnimann, C. E.; Ridenour, C. F.; Kinney, D. R.; Maciel, G. E., *J. Magn. Reson*. **1992**, *97*, 522–534
123. Lemaître, V.; Smith, M. E.; Watts, A., *Solid State Nucl. Magn. Reson*. **2004**, *26*, 215–235
124. Antzutkin, O. N.; Shekar, S. C.; Levitt, M. H., *J. Magn. Reson*. **1995**, *115*, 7–19
125. Dixon, W. T., *J. Chem. Phys*. **1982**, *77*, 1800–1807
126. Hu, J. Z.; Wang, W.; Liu, F.; Solum, M. S.; Alderman, D. W.; Pugmire, R. J.; Grant, D. M., *J. Magn. Reson*. **1995**, *113*, 210–222
127. Alderman, D. W.; McGeorge, G.; Hu, J. Z.; Pugmire, R. J.; Grant, D. M., *Mol. Phys*. **1998**, *95*, 1113–1126
128. Liu, S. F.; Mao, J. D.; Schmidt-Rohr, K., *J. Magn. Reson*. **2002**, *155*, 15–28
129. Tycko, R.; Dabbagh, G.; Mirau, P. A., *J. Magn. Reson*. **1989**, *85*, 265–274
130. Witter, R.; Hesse, St.; Sternberg, U., *J. Magn. Reson*. **2002**, *161*, 35–42
131. Chan, J. C. C.; Tycko, R., *J. Chem. Phys*. **2003**, 118, 8378–8389
132. Hodgkinson, P.; Emsley, L., *J. Chem. Phys*. **1997**, *107*, 4808–4816
133. Scheurer, C.; Skrynnikov, N. R.; Lienin, S. F.; Strays, S. K.; Bruschweiler, R.; Ernst, R. R., *J. Am. Chem. Soc*. **1999**, *121*, 4242–4251
134. Witter, R.; Hesse, S.; Sternberg, U., *J. Magn. Reson*. **2003**, *161*, 35–42
135. Witter, R.; Sternberg, U.; Ulrich, A. S., *J. Am. Chem. Soc*. **2006**, *128*, 2236–2243
136. Mason, J., *Solid State Nucl. Magn. Reson*. **1993**, *2*, 285–288
137. Xu, T.; Barich, D. H.; Torres, P. D.; Nicholas, J. B.; Haw, J. F., *J. Am. Chem. Soc*. **1997**, *119*, 396–405
138. Viswanathan, S.; Dadmun, M. D., *Macromolecules* **2003**, *36*, 3196–3205
139. Kuo, S. W.; Chang, F. C., *Macromolecules* **2001**, *34*, 7737–7743
140. Kuo, S. W.; Chan, S. C.; Chang, F. C., *Polymer (Guildf.)* **2002**, *43*, 3653–3660
141. Viswanathan, S.; Dadmun, M. D., *Macromolecules* **2002**, *35*, 5049–5060
142. Coleman, M. M.; Graf, J. F.; Painter, P. C., Specific interactions and the miscibility of polymer blends. Technomic Publishing: Lancaster, PA, **1991**
143. Kurosu, H.; Chen, Q., *Annu. Rep. NMR Spect*. **2004**, *52*, 167–200
144. Chu, P. P.; Wu, H. D., *Polymer (Guildf.)* **2000**, *41*, 101–109
145. Jiang, M.; Qiu, X.; Qin, W.; Fei, L., *Macromolecules* **1995**, *28*, 730–735
146. Ward, I. M.; Hadley, D. W., An Introduction to the Mechanical properties of solid polymers, Chichester; New York: J. Wiley & Sons, **1993**
147. Schmidt-Rohr, K., Spiess, H. W., Multidimensional Solid-State NMR and Polymers. *Academic Press Inc.: San Diego, CA*, **1994**
148. Schaefer, J.; McKay, R. A.; Stejskal, E. O.; Dixon, W. T., *J. Magn. Reson*. **1983**, *52*, 123–129
149. Schaefer, J.; Sefcik, M. D.; Stejskal, E. O.; McKay, R. A.; Dixon, W. T.; Cais, R. E., *Macromolecules* **1984**, *17*, 1107–1118
150. Spiess, H. W., *Colloid Polym. Sci*. **1983**, *261*, 193–209
151. Wu, C. H.; Ramamoorthy, A.; Opella, J. S., *J. Magn. Reson. A* **1994**, *109*, 270–272
152. Spiess, H. W., edited by H. H. Kausch and H.G. Zachmann ~Springer, Berlin, *in Adv. olym. Sci*, **1985**, *66*, 24–57
153. Schaefer, J.; Sefcik, M. D.; Stejskal, E. O.; McKay, R. A., *Macromolecules* **1984**, *17*, 1118–1124
154. Jack, K. S.; Whittaker, A. K., *Macromolecules* **1997**, *30*, 3560–3568
155. Simon, G.; Baumann, K.; Gronski, W., *Macromolecules* **1992**, *25*, 3624–3628
156. Kariyo, S.; Stapf, S., *Macromolecules* **2002**, *35*, 9253–9255
157. Kimmich, R.; Fatkullin, N., *Adv. Polym. Sci*. **2004**, *170*, 1–113
158. Min, B.; Qiu, X.; Ediger, M. D.; Pitsikalis, M.; Hadjichristidis, N., *Macromolecules* **2001**, *34*, 4466–4475
159. Hischinger, J.; Kranig, W.; Spiess, H. W., *Colloid Polym. Sci*. **1991**, *269*, 993–1002
160. Haeberlen, U., High Resolution NMR in Solids, Suppl. 1 to Advances in Magnetic Resonance, Academic Press, New York, **1976**
161. Fortier-McGill, B.; Toader, V.; Reven, L., *Macromolecules* **2011**, *44*, 2755–2765
162. Haraguchi, K.; Takehisa, T.; Fan, S., *Macromolecules* **2002**, *35*, 10162–10171
163. Cao, X.; Lee, L. J.; Widya, T.; Macosko, C., *Polymer (Guildf.)* **2005**, *46*, 755–783
164. Modesti, M.; Lorenzetti, A.; Besco, S.; Hrelja, D.; Semenzato, S.; Bertani, R.; Michelin, R. A., *Polym. Degrad. Stabil*. **2008**, *93*, 2166–2171
165. Wang, M.; Bertmer, M.; Demco, D. E.; Blumich, B.; Litvinov, V. M.; Barthel, H., *Macromolecules* **2003**, *36*, 4411–4413
166. Traer, J. W.; Goward, G. R., *Magn. Reson. Chem*. **2007**, *45*, S135–S143
167. Schnell, I.; Brown, S. P.; Low, H. Y.; Ishida, H.; Spiess, H. W., *J. Am. Chem. Soc*. **1998**, *120*, 11784–11795

168. Mirau, P. A.; White, J. L., *Macromolecules* **1994**, *27*, 1648–1650
169. Zhang, X. Q.; Takegoshi, K.; Hikichi, K., *Macromoleculaes* **1991**, *24*, 5756–5762
170. Gu, Z. T.; Zambrano, R.; McDermott, A., *J. Am. Chem. Soc*. **1994**, *116*, 6368–6372
171. Aliev, A. E.; Harris, K. D. M.; Shannon, I. J.; Glidewell, C.; Zakaria, C. M.; Schofield, P. A., *J. Phys. Chem. B* **1995**, *99*, 12008–12015
172. Wu, C. H.; Ramamoorthy, A.; Opella, S., *J. Magn. Reson. A* **1994**, *109*, 270–272
173. Marassi, F. M.; Ma, C.; Gesell, J. J.; Opella, S. J., *J. Magn. Reson*. **2000**, *144*, 156–161
174. Wang, J.; Kim, S.; Kovacs, F.; Cross, T. A., *Protein Sci*. **2001**, *10*, 2241–2250
175. Dvinskich, S. V.; Zimmermann, H.; Maliniak, A.; Sandstrom, D., *J. Magn. Reson*. **2003**, *164*, 165–170
176. Huang, H.; Malkov, S.; Coleman, M. M.; Painter, P. C., *Appl. Spectrosc*. **2004**, *58*, 1074–1081
177. Schmidt-Rohr, K.; Kulik, A. S.; Beckham, H. W.; Ohlemacher, A.; Pawelzik, U.; Boeffel, C.; Spiess, H. W., *Macromolecules* **1994**, *27*, 4733–4745